Extended Data for "The Effect of Large-Scale Anti-Contagion Policies on the Coronavirus (COVID-19) Pandemic"

Solomon Hsiang,*[1,2] Daniel Allen,[†1] Sébastien Annan-Phan,[†1,3] Kendon Bell,[†1,4] Ian Bolliger,[†1,5] Trinetta Chong,[†1] Hannah Druckenmiller,[†1,3] Luna Yue Huang,[†1,3] Andrew Hultgren,[†1,3] Emma Krasovich,[†1] Peiley Lau,[†1,3] Jaecheol Lee,[†1,3] Esther Rolf,[†1,6] Jeanette Tseng,[†1] and Tiffany Wu[†1]

[1]Global Policy Laboratory, Goldman School of Public Policy, UC Berkeley
[2]National Bureau of Economic Research & Centre for Economic Policy Research
[3]Agricultural & Resource Economics, UC Berkeley
[4]Manaaki Whenua – Landcare Research
[5]Energy & Resources Group, UC Berkeley
[6]Electrical Engineering & Computer Science Department, UC Berkeley

*Correspondence: shsiang@berkeley.edu. [†] Equal contribution (alphabetical).

All data and code are available at https://github.com/bolliger32/gpl-covid.
Additional resources and updates are available at www.globalpolicy.science/covid19.
For repository related questions, please contact bolliger@berkeley.edu.
For data related questions, please contact peiley@berkeley.edu.

This document last updated: April 20, 2020. Data last updated: April , 2020.

a

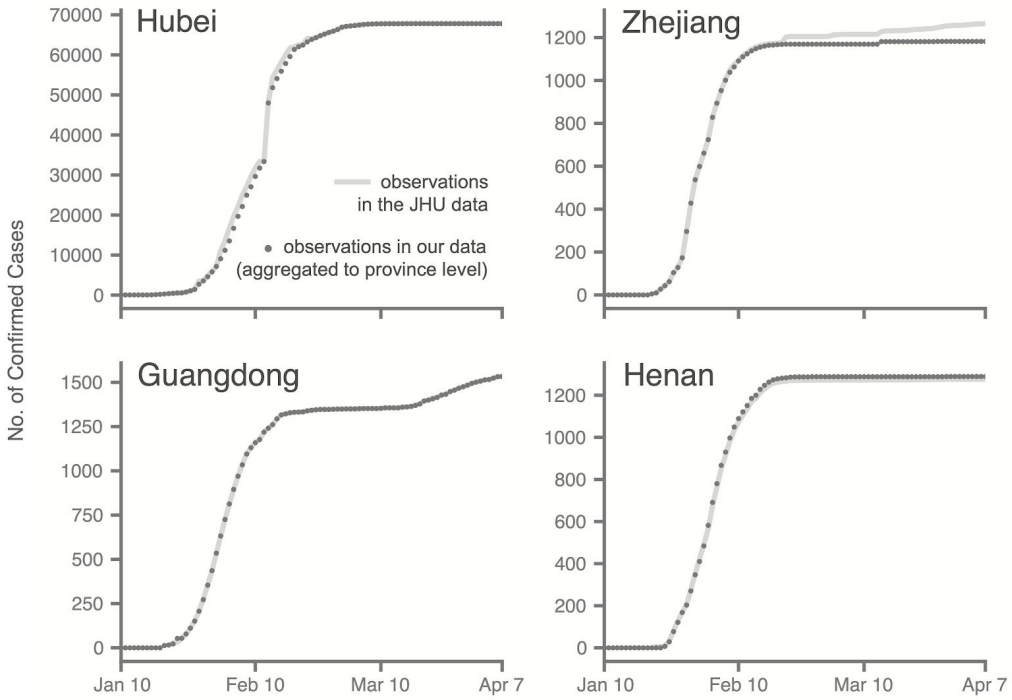

b

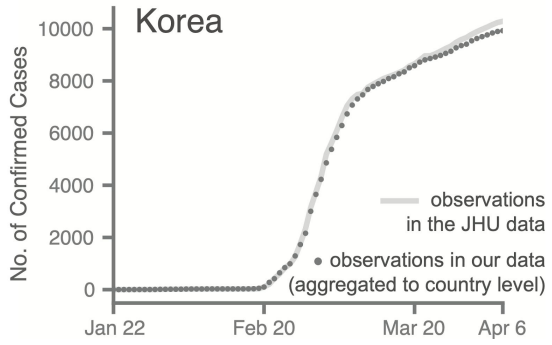

Extended Data Figure 1 | Validating disaggregated epidemiological data against aggregated data from the Johns Hopkins Center for Systems Science and Engineering. Comparison of cumulative confirmed cases from a subset of regions in our collated epidemiological dataset to the same statistics from the 2019 Novel Coronavirus COVID-19 (2019-nCoV) Data Repository by the Johns Hopkins Center for Systems Science and Engineering (JHU CSSE).[1] We conduct this comparison for Chinese provinces and South Korea, where the data we collect are from local administrative units that are more spatially granular than the data in the JHU CSSE database. **a,** In China, we aggregate our city-level data to the province level, and **b,** in Korea we aggregate province-level data up to the country level. Small discrepancies, especially in later periods of the outbreak, are generally due to imported cases (international or domestic) that are present in national statistics but which we do not assign to particular cities (in China) or provinces (in Korea).

1 https://github.com/CSSEGISandData/COVID-19 (access date: April 7, 2020)

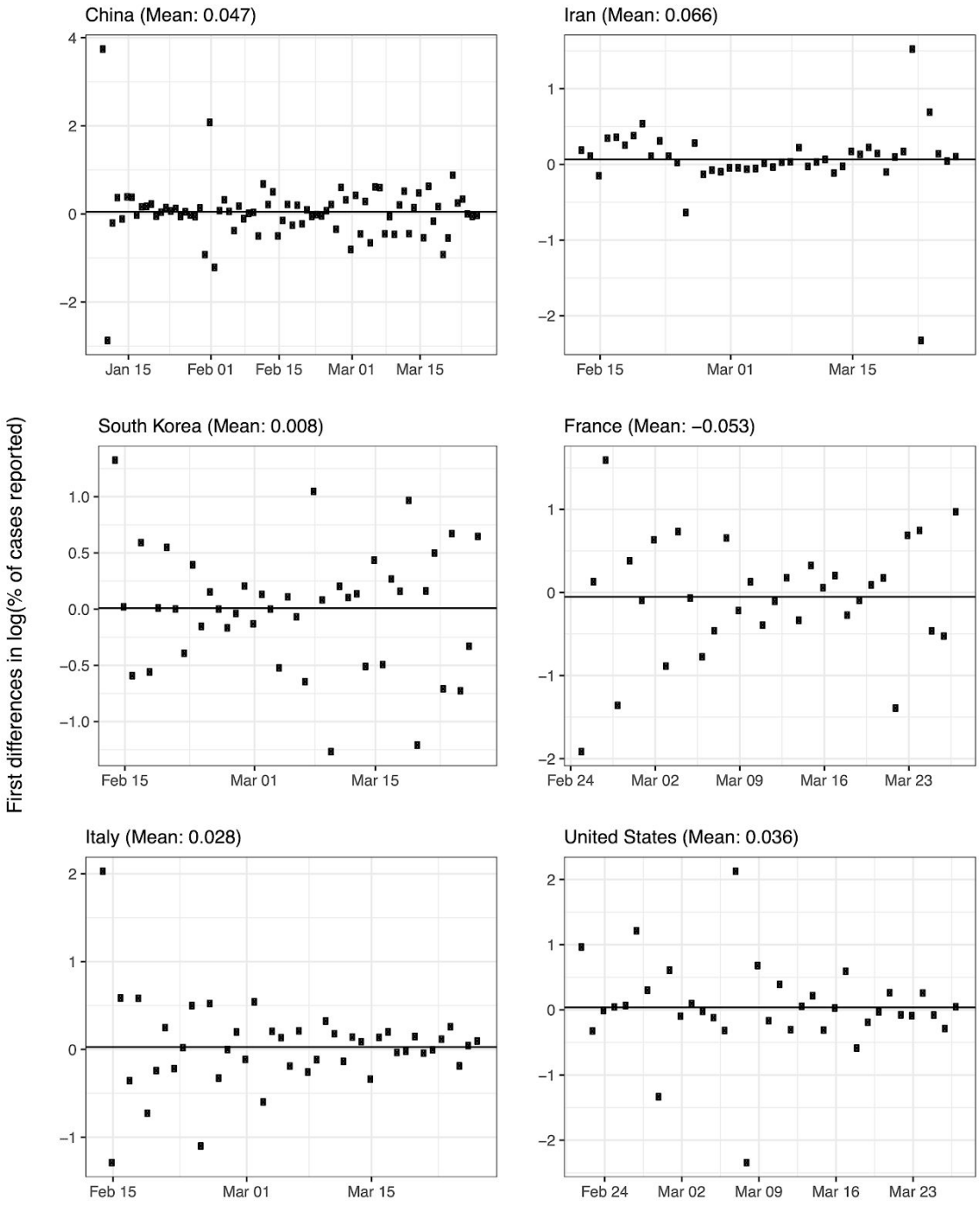

Extended Data Figure 2 | Estimated trends in case detection over time within each country. Systematic trends in case detection may potentially bias estimates of no-policy infection growth rates (see Equation 8). We estimate the potential magnitude of this bias using data from the Centre for Mathematical Modelling of Infectious Diseases.[2] Markers indicate daily first-differences in the logarithm of the fraction of estimated symptomatic cases reported for each country over time. The average value over time (solid line and value denoted in panel title) is the average growth rate of case detection, equal to the magnitude of the potential bias. For example, in the main text we estimate that the infection growth rate in the United States is 0.30 (Figure 2A), of which growth in case detection might contribute 0.036 (this figure).

[2] Russell, T., Joel Hellewell, and S. Abbot. "Using a delay-adjusted case fatality ratio to estimate under-reporting." *Centre for Mathematical Modelling of Infectious Diseases Repository* (2020). URL: https://cmmid.github.io/topics/covid19/severity/global_cfr_estimates.html (access date: April 18, 2020)

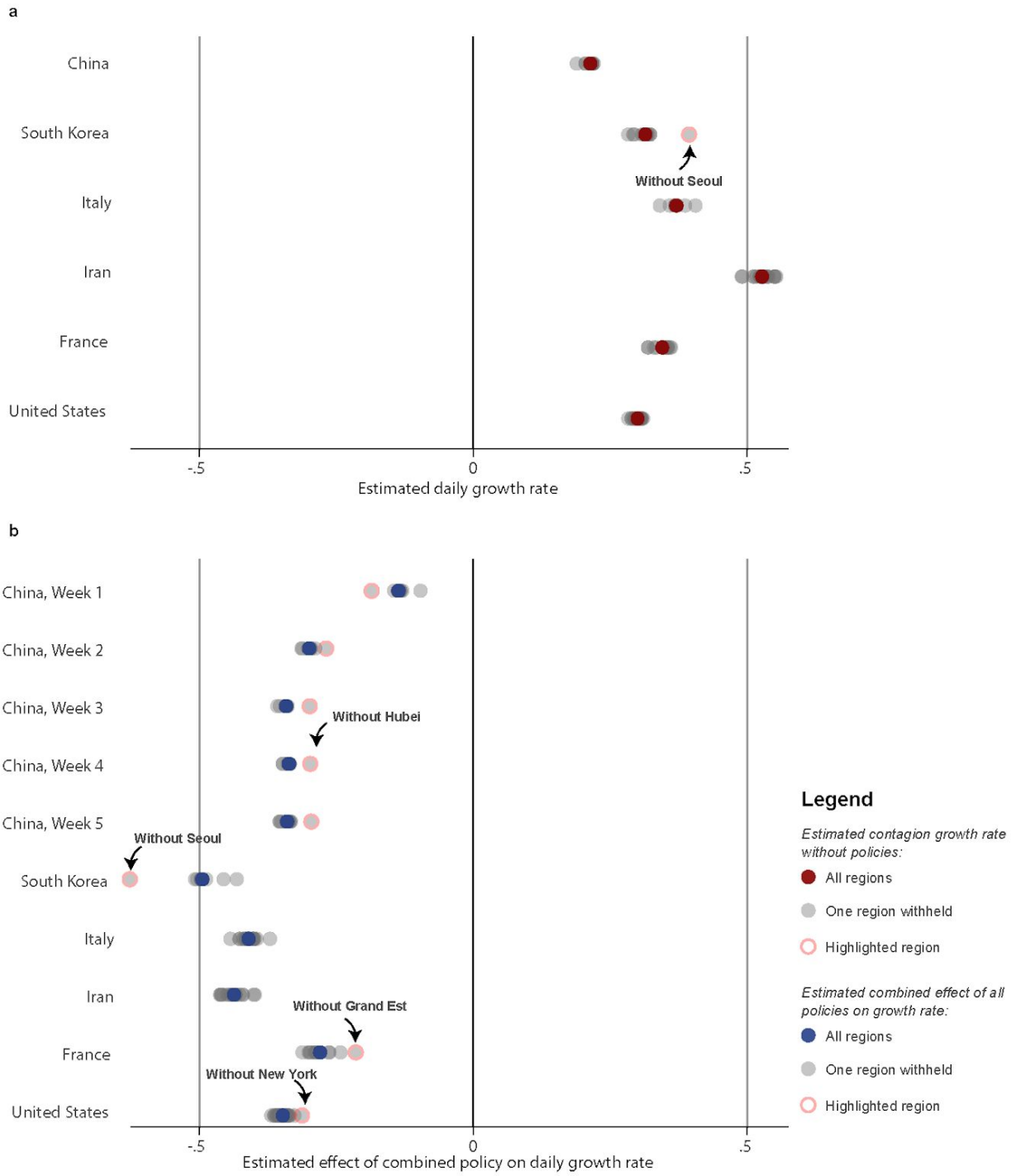

Extended Data Figure 3 | Robustness of the estimated no-policy growth rate of infections and the combined effect of policies to withholding blocks of data from entire regions. For each country, we re-estimated Eq. 7 using real data *k* times, each time withholding one of the *k* first-level administrative regions ("Adm1," i.e. state or province) in that country. Each gray circle is either (**a**) the estimated no-policy growth rate or (**b**) the total effect of all policies combined, from one of these *k* regressions. Red and blue circles show estimates from the full sample, identical to results presented in panels A and B of Figure 2, respectively. For each country panel, if a single region is influential, the estimated value when it is withheld from the sample will appear as an outlier. Some regions that appear influential are highlighted with an open pink circle. As in Figure 2B of the main text, we estimate a distributed lag model for China and display each of the estimated weekly lag effects (red circle is the same "without Hubei" sample for lags).

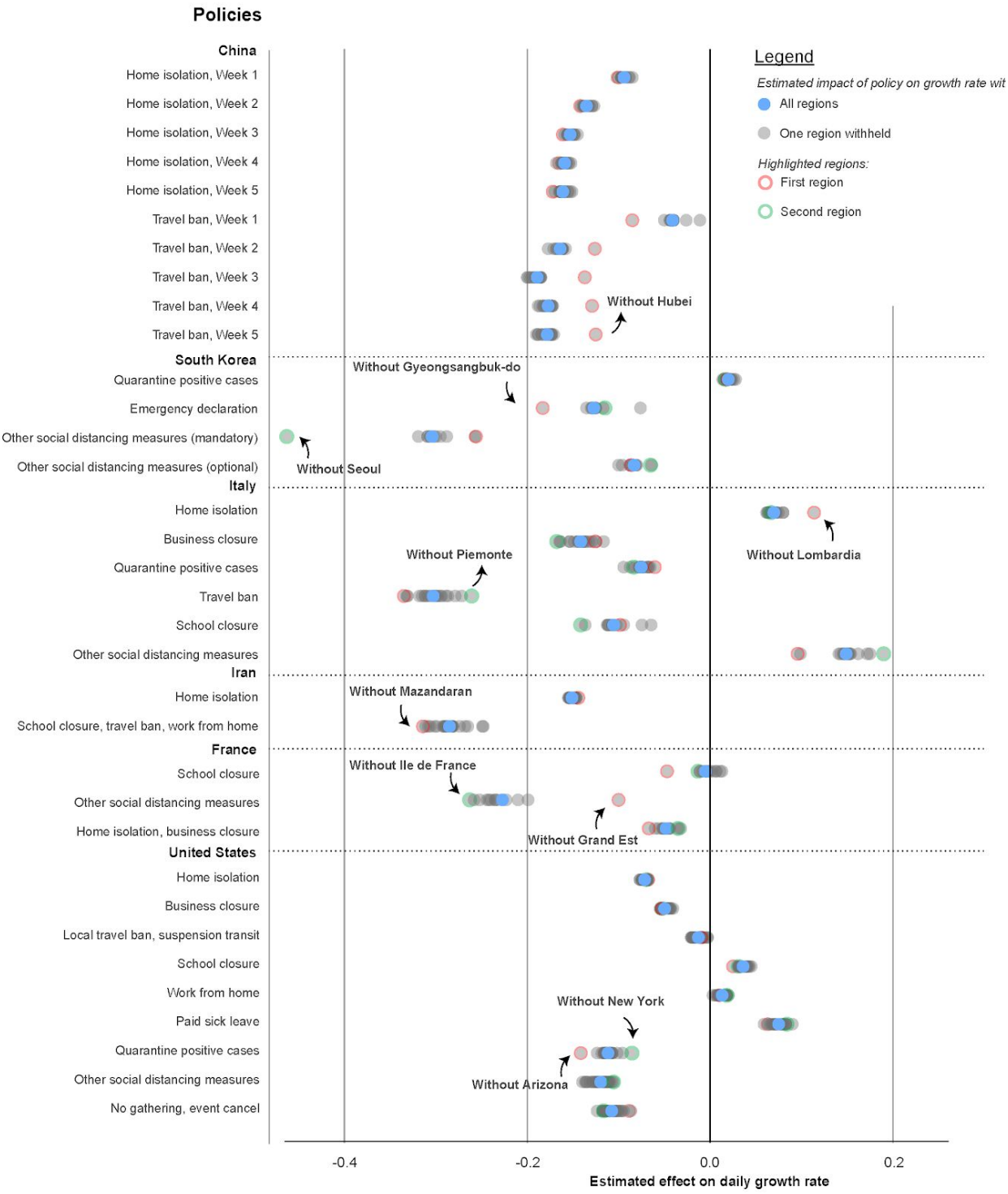

Extended Data Figure 4 | Robustness of the estimated effects of individual policies to withholding blocks of data from entire regions. Same as Extended Data Figure 3, but for individual policies (analogous to Figure 2C in the main text). In cases where two regions are influential, a second region is highlighted with an open green circle.

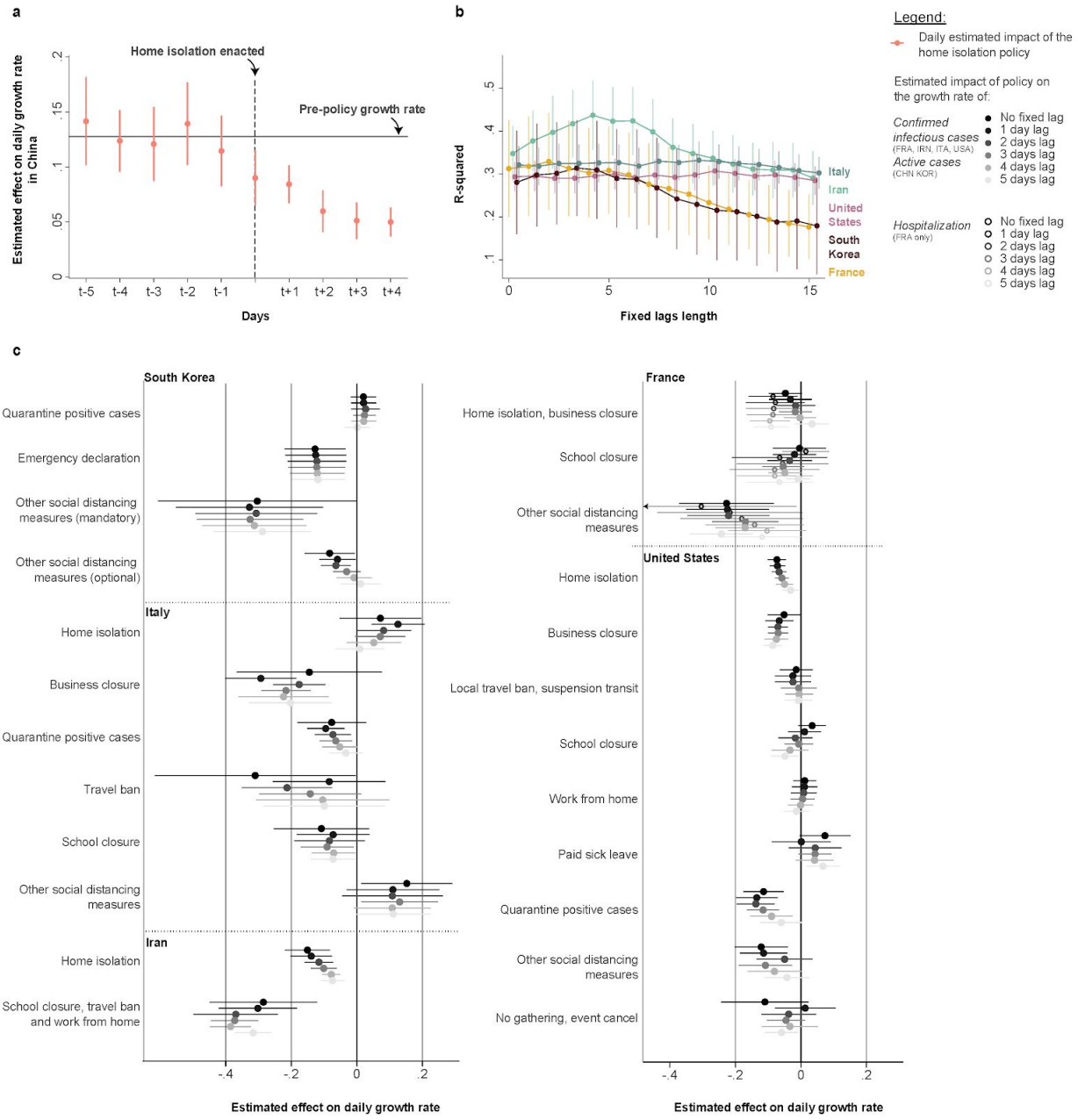

Extended Data Figure 5 | Evidence supporting models where policies affect infection growth rates in the days following deployment. Existing evidence has not demonstrated whether policies should affect infection growth rates in the days immediately following deployment. It is therefore not clear *ex ante* whether the policy variables in Eq. 7 should be encoded as "on" immediately following a policy deployment. We estimate "fixed-lag" models in which a fixed delay between a policy's deployment and its effect is assumed (see Supplementary Methods 3). If a delay model is more consistent with real world infection dynamics, these fixed lag models should recover larger estimates for the impact of policies and exhibit better model fit. **a**, Because data from China cover a longer period with fewer policies that are each implemented early in the sample, we estimated an explicit distributed lag model in the main article (Figure 2), finding evidence of policy impacts in the first week of deployment and evidence that these effects increase in the following weeks. Using a reduced sample of 36 Chinese cities where at least five days of infection data are available before and after the first policy (*home isolation*) is deployed, we implement an event study.[3] Orange markers show the average infection growth rate in the five days immediately prior to and following the first policy deployment. **b**, R-squared values associated with fixed-lag lengths varying from zero to fifteen days. In-sample fit generally declines or remains unchanged if policies are assumed to have a delay longer than four days (whiskers are 95% CI computed through resampling). **c**, Estimated effects for no lag (the model reported in the main text) and for fixed-lags between one and five days. Estimates generally are unchanged or shrink towards zero (e.g. *Home isolation* in Iran), consistent with mis-coding of post-policy days as no-policy days.

[3] For a canonical example, see: Jacobson, L. S., LaLonde, R. J., & Sullivan, D. G. (1993). Earnings losses of displaced workers. *The American Economic Review*, 685-709.

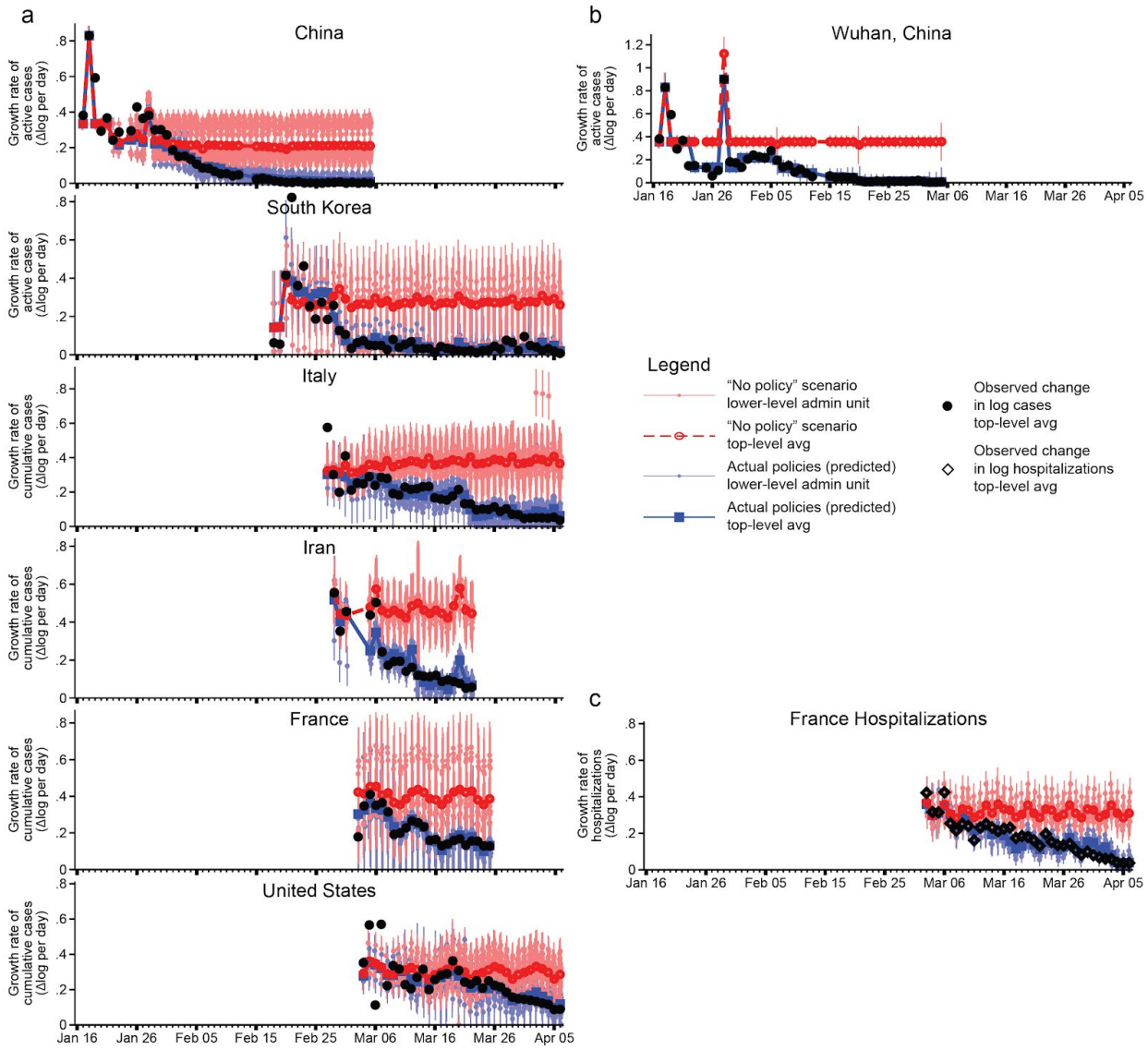

Extended Data Figure 6 | Estimated infection or hospitalization growth rates with actual anti-contagion policies and in a "no policy" counterfactual scenario. a, The estimated daily growth rates of active (China, South Korea) or cumulative (all others) infections based on the observed timing of all policy deployments within each subnational unit (blue) and in a scenario where no policies were deployed (red). Identical to Figure 3 in the main text, but using an alternative disaggregated encoding of policies that does not group any policies into policy packages. **b**, Same as Figure 3 in the main text, but Eq. 7 is implemented for a single example administrative unit, Wuhan, China. **c**, Same as Figure 3 in the main text, but using hospitalization data from France rather than cumulative cases, since the French government stopped reporting the latter after March 25, 2020. For all panels, the difference between the with- and no-policy predictions is our estimated effect of actual anti-contagion policies on the growth rate of infections (or hospitalizations). The markers are daily estimates for each subnational administrative unit (vertical lines are 95% confidence intervals). Black circles are observed changes in log(*infections*) (or diamonds for log(*hospitalizations*)), averaged across the same administrative unit.

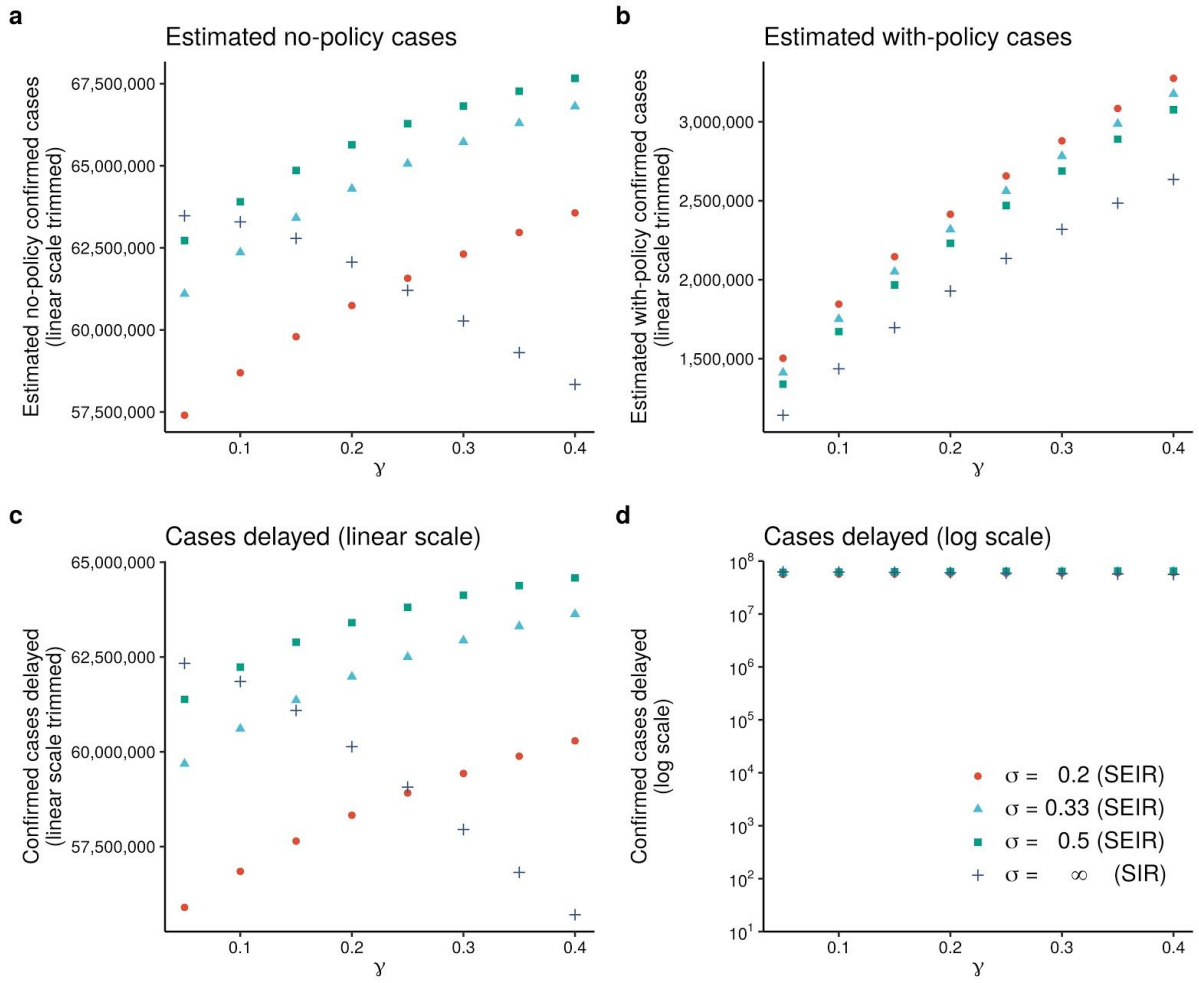

Extended Data Figure 7 | Sensitivity of estimated averted/delayed infections to the choice of γ and σ in an SIR/SEIR framework. This figure displays the sensitivity of total averted/delayed cases presented in Figure 4 of the main text to alternative modeling assumptions. We compute total cases across the respective final days in our samples for the six countries presented in our analysis. The figure displays how these totals vary with eight values of γ (0.05-0.4) and four values of σ (0.2, 0.33, 0.5, ∞), where the final value of σ (∞) corresponds to the SIR model. **a**, The simulated total number of infections under no policy. **b**, Same, but using actual policies. **c**, The difference between (**a**) and (**b**), which are the total number of averted/delayed infections. **d**, Same as (**c**), but on a logarithmic scale similar to Figure 4 in the main text (**a**-**c** are on a linear scale, trimmed to show details). Figure 4 in the main text uses γ = 0.079, which we calculate using empirical recovery/death rates in countries where we observe them (China and South Korea, see Methods). If we assume a 14-day delay between infected individuals becoming non-infectious and being reported as "recovered" in the data, we would calculate γ = 0.18. Figure 4 in the main text assumes $\sigma = \infty$.

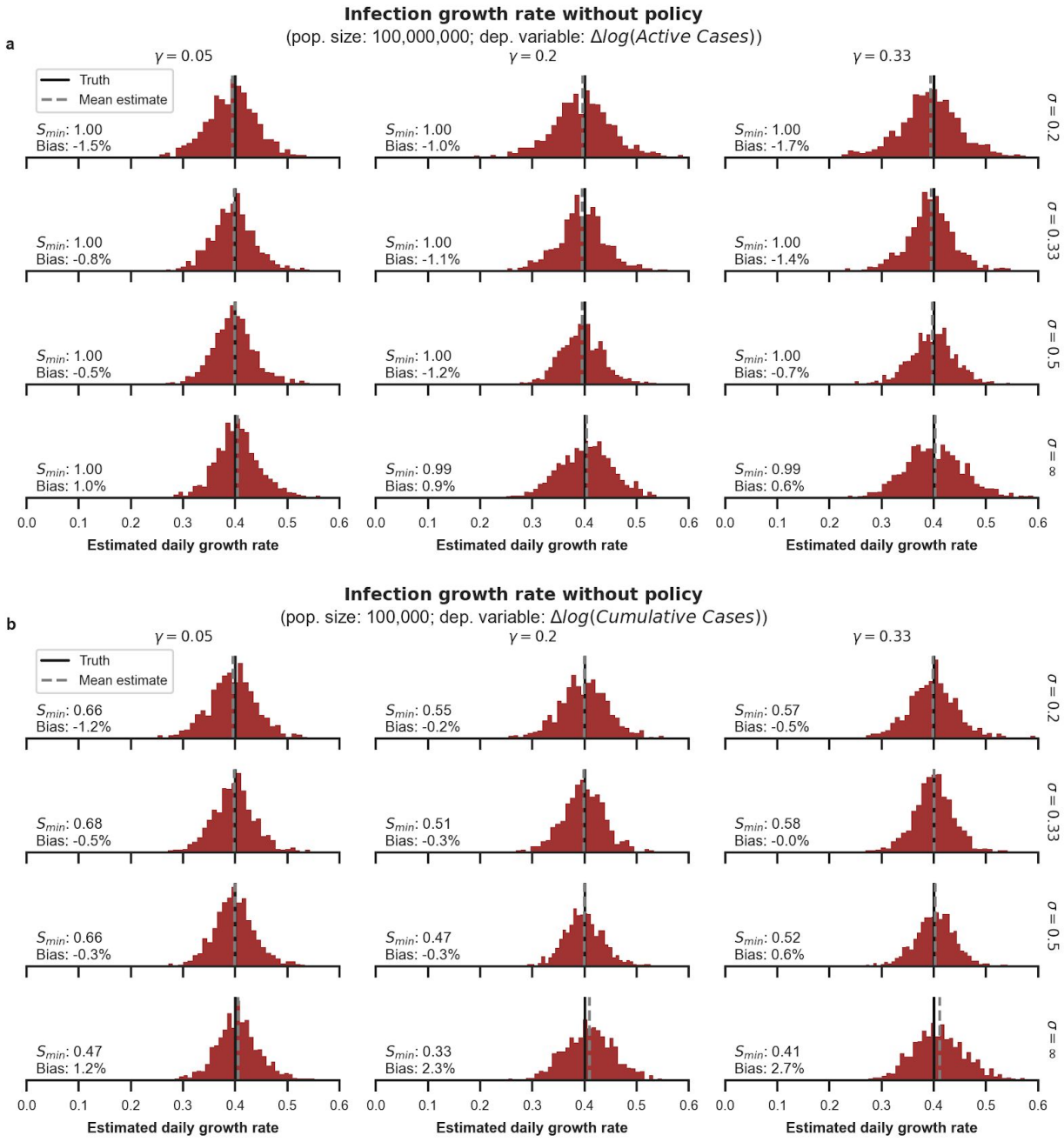

Extended Data Figure 8 | Simulating reduced form estimates for the no-policy growth rate of infections for different population regimes and disease dynamics. We examine the performance of reduced form econometric estimators through simulations in which different underlying disease dynamics are assumed (see Supplementary Information Section 3). Each histogram shows the distribution of econometrically estimated values across 1,000 simulated outbreaks. Estimates are for the no-policy infection growth rate (analogous to Figure 2A) when three different policies are deployed at random moments in time. The black line shows the correct value imposed on the simulation and the red histogram shows the distribution of estimates using the regression in Eq. 7, applied to data output from the simulation. The grey dashed line shows the mean of this distribution. The 12 subpanels describe the results when various values are assigned to the mean latency period (γ^{-1}) and mean infectious period (σ^{-1}) of the disease. "$\sigma = \infty$" is equivalent to SIR disease dynamics. In each panel, S_{min} is the minimum susceptible fraction observed across all 1,000 45-day simulations shown in each panel. For reference, in the real datasets used in the main text, after correcting for country-specific underreporting, S_{min} across all units analyzed is 0.78 and 95% of the analyzed units finish with $S_{min} > 0.93$. "Bias" refers to the distance between the dashed grey and black line as a percentage of the true value. **a**, Simulations in near-ideal data conditions in which we observe active infections within a large population (such that the susceptible fraction of the population remains high during the sample period). For example, these conditions are similar to those in our real data for Chongqing, China. **b**, Simulations in a non-ideal data scenario where we are only able to observe cumulative infections in a small population. For example, these conditions are similar to those in our real sample of data for Cremona, Italy.

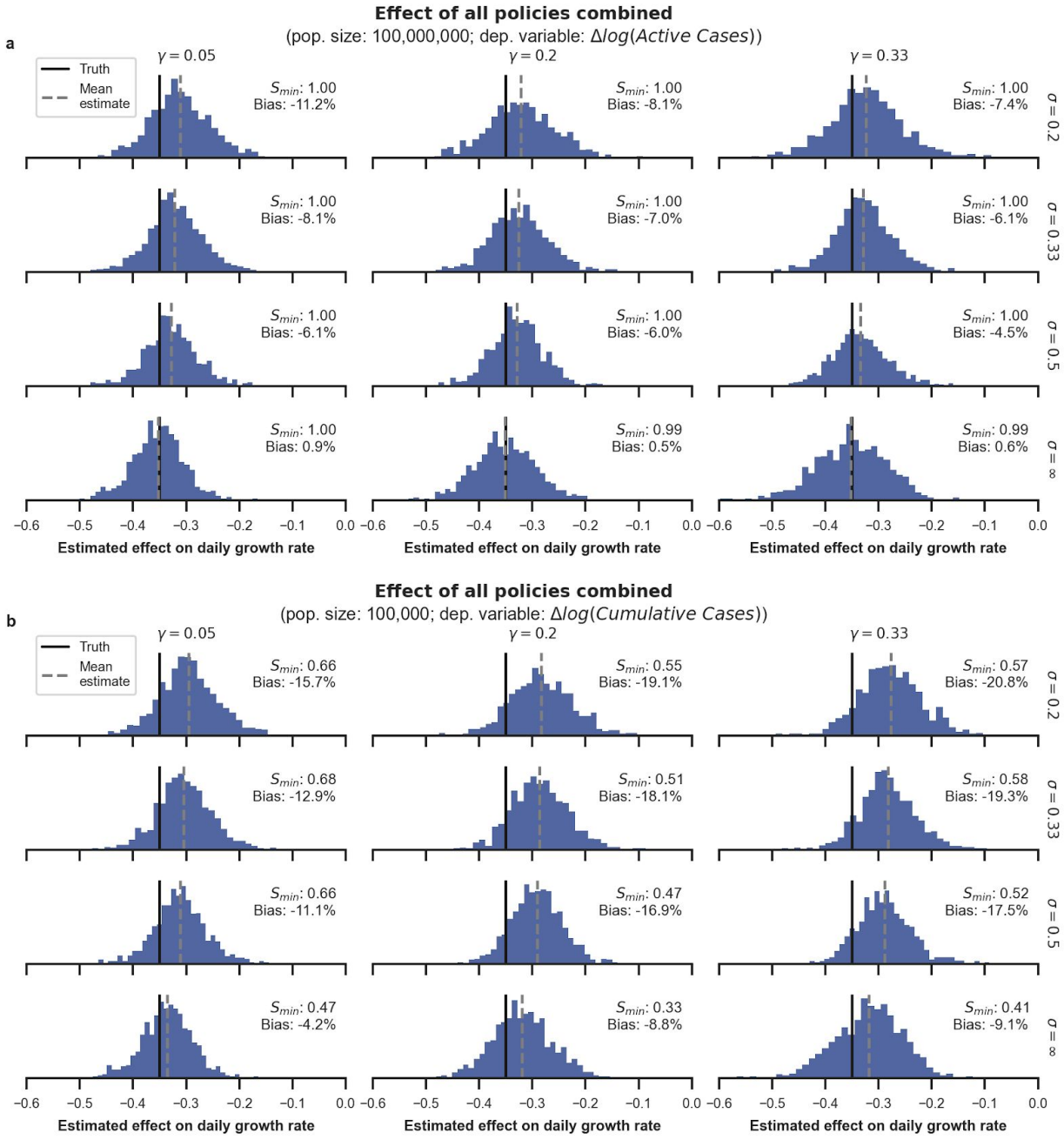

Extended Data Figure 9 | Simulating reduced form estimates for anti-contagion policy effects for different population regimes and assumed disease dynamics. Same as Extended Data Figure 8, but estimates are for the combined effect of three different policies (analogous to Figure 2B) that are deployed at random moments in time.

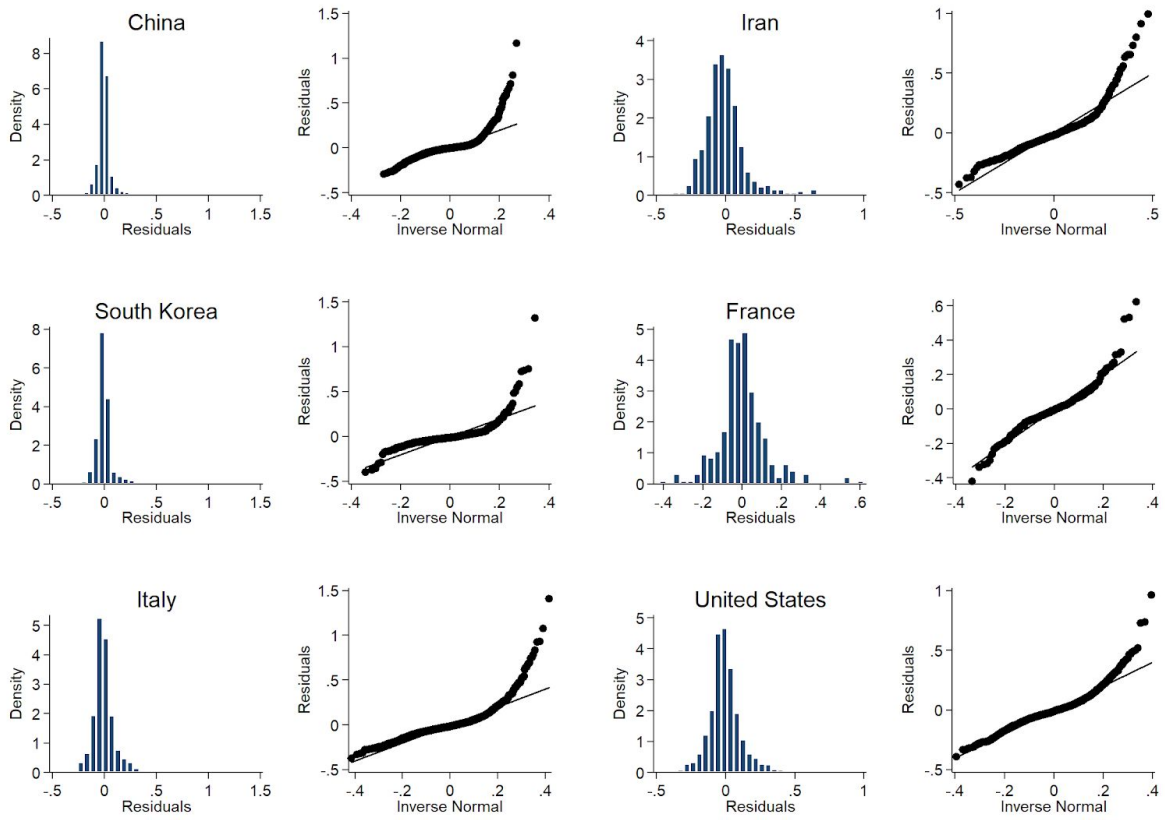

Extended Data Figure 10 | Regression residuals for the growth rates of COVID-19 by country. These plots show the estimated residuals from Equation 7 for each country-specific econometric model. Histograms (left) show the estimated unconditional probability density function. Quantile plots (right) show quantiles of the cumulative density function (y-axis) plotted against the same quantiles for a Normal Distribution. For additional details, see the full model under the Methods - Econometric analysis section as well as the results in Figure 3 of the main paper.